

Theory of impurity effects on electron heat transport driven by micro-tearing mode in the pedestal of plasmas

Shanni Huang, Weixin Guo* and Lu Wang*

International Joint Research Laboratory of Magnetic Confinement Fusion and Plasma Physics, State Key Laboratory of Advanced Electromagnetic Technology, Huazhong University of Science and Technology

Abstract

The impurity-modified dispersion relation of micro-tearing mode (MTM), which has been identified as the dominant instability in the DIII-D strong-gradient pedestal region, and the corresponding electron heat flux are derived. The associated effective electron heat conductivity is then calculated using quasi-linear theory. Parametric dependence analysis shows that in fixed $Z_{\text{eff}} = 1.2$, increasing the impurity charge number can suppress the electron heat transport, mainly due to the reduction of the fluctuation amplitude. In contrast, steepening the full ionized impurity density profile can enhance the electron heat transport by increasing the growth rate of MTM. These results can provide a theoretical reference for understanding the physical mechanism of electron heat transport in the pedestal region.

1. Introduction

Pedestal transport is important for H-mode confinement. Studies on DIII-D, JET and EAST have suggested that micro-tearing modes (MTMs) can dominate pedestal electron heat transport ^[1-3]. On the other hand, impurities are unavoidable. Non-trace impurities may modify both MTM instability and the associated turbulent transport in the pedestal. First, the inclusion of impurity can increase the collisionality, which is considered as one of the driving factors of MTM ^[4]. Second, changes in the impurity profile can modify η_i through dilution effects and thereby affect MTM instability ^[5]. However, the effects of impurity-induced changes in collisionality and dilution effects on electron heat transport driven by MTM in the pedestal remain unclear, and are therefore investigated in this work.

2. Derivation of the MTM instability and the heat flux driven by MTM in the DIII-D strong gradient pedestal

In this section, we will perform the analytical derivation based on the orderings calculated from the DIII-D H-mode strong gradient pedestal parameters [6]. The perturbed electron density and ion/impurity density are obtained from the drift-kinetic equation and the gyrokinetic equation, respectively. And substituting the perturbed particle densities of all species into the quasi-neutrality condition $\delta n_e = \delta n_i + Z\delta n_z$, the MTM eigen-equation with impurity is then obtained. Since the DIII-D strong-gradient pedestal parameters satisfy $\omega < v_{ei}$ and $\omega < \frac{k_{\parallel}^2 v_{the}^2}{v_{ei}}$, the eigen-equation can be solved

using semi-collisional theory [7-8]. The real frequency and growth rate of MTM are:

$$\hat{\omega}_r = 1 + \frac{2}{\rho_{\text{eff,cs}}^2 / \rho_{\text{cs}}^2 + K_{\text{eff}}} \left(\frac{1}{\hat{\beta}_e |\Delta' \rho_{\text{cs}}|} \right)^2 - \frac{2\sqrt{2Z_{\text{eff}} \hat{v}_{e0} \eta_e}}{\hat{\beta}_e^{3/2} |\Delta' \rho_{\text{cs}}| (\rho_{\text{eff,cs}}^2 / \rho_{\text{cs}}^2 + K_{\text{eff}})} C_{v\eta} \quad (1)$$

$$\hat{\gamma} = 4 \frac{\sqrt{Z_{\text{eff}} \hat{v}_{e0} \eta_e}}{\hat{\beta}_e |\Delta' \rho_{\text{cs}}| (\rho_{\text{eff,cs}}^2 / \rho_{\text{cs}}^2 + K_{\text{eff}})} C_{v\eta} \left(1 - \sqrt{2Z_{\text{eff}} \hat{v}_{e0} \eta_e} |\Delta' \rho_{\text{cs}}| \hat{\beta}_e C_{v\eta} \right) \quad (2)$$

where $\rho_{\text{eff,cs}}^2 / \rho_{\text{cs}}^2 = f_i + (m_z / m_i) f_c$ represents the impurity-modified effective inertia

factor normalized to the main-ion sound gyro-radius, $K_{\text{eff}} = \sum_{s=i,z} \frac{m_s}{m_i} \frac{f_s}{Z_s} \frac{1}{Z_s \tau_s} \frac{L_{ne}}{L_{ns}} (1 + \eta_s)$

is the impurity-modified effective MTM drive associated with the equilibrium density and temperature gradients, $Z_{\text{eff}} = \sum_{s=i,z} f_s Z_s$ is the effective charge number,

$C_{v\eta} = \left(\frac{1.71}{d_1} \right)^{1/2} \sqrt{\frac{\hat{\omega}_{*e}}{2}} \frac{1}{k_y \rho_{\text{cs}}} \frac{L_s}{a} \sqrt{\frac{m_e}{m_i}}$ is a constant relative to η_e , $\hat{\omega}_{*e} = \frac{\omega_{*e}}{c_s / a}$, $\Delta' = -2k_y$

is micro-tearing stability parameter [9].

Based on the quasi-linear theory, the expression of the radial electron heat flux can be further obtained by substituting the perturbed electron distribution function into the heat flux, and the total electron heat-conductivity expression is obtained as follows:

$$\chi_e^{\text{eff}} = \chi_{\phi\phi}^{\text{eff}} + \chi_{AA}^{\text{eff}} = \left[\frac{33}{4} \frac{\gamma_k}{(\omega_r)^2} + 3 \frac{\gamma_k}{(\omega_r + \omega_s)^2} \right] (k_{\theta} \rho_{\text{cs}} c_s)^2 |\delta\hat{\phi}_k|^2 \quad (3)$$

where $\omega_s = -k_\perp^2 d_e^2 k_\parallel^2 v_{the}^2 \left[\omega_r - \omega_{*e} \left(1 + \frac{3}{2} \eta_e \right) \right]^{-1}$, $\chi_{\phi\phi}^{eff}$ is the electrostatic contribution,

χ_{AA}^{eff} is the electromagnetic contribution. Noticed that no mixed $\chi_{\phi A}^{eff}$ term appears in the final equation (4), because it is entirely contributed by the particle-convection part of the energy flux and are therefore cancelled after subtracting the convective energy flux. In addition, using Ampère's law and Poisson's equation, the perturbed electrostatic potential and radial magnetic perturbation can be related as

$$|\delta\hat{\phi}| = \frac{e}{T_e} \left| \frac{\omega_s + \omega}{k_\theta k_\parallel} \right| \delta B_r,$$

where $\delta B_r = 12$ Gauss [6].

3. Impurity effects on the electron heat conductivity driven by MTM in the DIII-D strong gradient pedestal

In this section, the parametric dependences of both MTM instability and electron heat transport driven by MTM will be analyzed in detail based on the analytical results in Sec. 2. The dependence of MTM-driven electron heat transport on the impurity density profile is further analyzed. With the electron density gradient fixed at $a/L_{ne} = 17.1$ and the effective charge fixed at $Z_{eff} = 1.2$, the effective electron heat conductivity versus \hat{L}_{ez} in the presence of fully ionized He²⁺ and Ne¹⁰⁺ impurities is shown in Figs. 1(a) and 1(b), respectively. Compared with the Ne¹⁰⁺ case, the increase of the effective electron heat conductivity is more evident than which in He²⁺ case, which is consistent with the stronger variation of the corresponding ω_r and γ , as shown in Figs. 1(c) and 1(d). Moreover, it can be seen that $\chi_{\phi\phi}^{eff}$, χ_{AA}^{eff} , and the total χ_e^{eff} all increase with the increase of \hat{L}_{ez} . This is because ω_r varies only weakly, while γ increases with larger \hat{L}_{ez} .

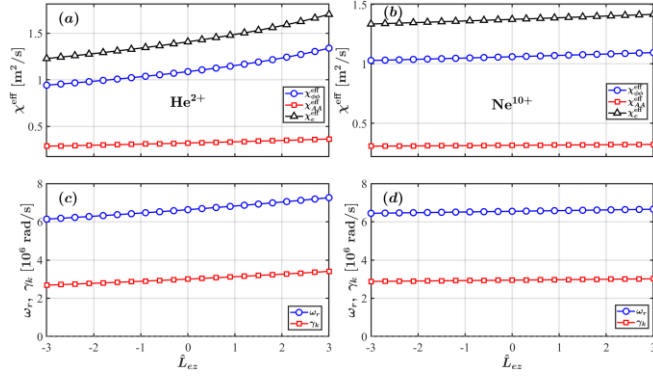


Fig. 1 The effective electron heat conductivity versus \hat{L}_{ez} in the presence of (a) He^{2+} and (b) Ne^{10+} impurities, respectively. Blue lines represent $\chi_{\phi\phi}^{\text{eff}}$, red lines represent χ_{AA}^{eff} , and black lines represent χ_e^{eff} . ω_r (blue lines) and γ (red lines) of MTM instability versus \hat{L}_{ez} in the presence of (c) He^{2+} and (d) Ne^{10+} impurities, respectively. $T_{0z} = T_{0i}$, $\hat{L}_{ez} = 1$.

4. Summary and Acknowledgments

In this work, the impurity-modified dispersion relation of MTM and the associated effective electron heat conductivity are derived. The increase of impurity charge number tends to suppress the electron heat transport. In contrast, steepening the negative impurity density gradient can enhance the electron heat transport. These results indicate that impurity parameters can modulate MTM instability and the associated electron heat transport, and may provide a theoretical reference for understanding the mechanism of electron heat transport in the pedestal region.

This work was supported by the National MCF Energy R&D Program of China under Grant No. 2024YFE03060001, and the National Natural Science Foundation of China under Grant Nos. 12275096 and 12275097.

References

- [1] Yan, et al, *Nucl. Fusion*, **64** (2024) 096001
- [2] Hatch, et al, *Nucl. Fusion*, **61** (2021) 036015
- [3] Qu, et al, *Radiat. Eff. Defects Solids*, **179** (2024) 514
- [4] Chen, et al, *Nucl. Fusion*, **63** (2024) 066019
- [5] Xie, et al, *Phys. Plasmas*, **30** (2023) 082111
- [6] Curie, et al, *Nucl. Fusion*, **62** (2022) 126061
- [7] Connor, et al, *Plasma Phys. Control. Fusion*, **54** (2012) 035003
- [8] Zocco, et al, *Plasma Phys. Control. Fusion*, **57** (2015) 065008
- [9] Hamed, et al, *Phys. Plasmas*, **30** (2023) 042303